AFRL-ML-WP-TP-2004-402

THE GROWTH AND CHARACTERIZATION OF PHOTONIC THIN FILMS

S. Tullis, W.E. Johnson, K. Eyink, P. Fleitz, and T.J. Bunning

Hardened Materials Branch (AFRL/MLPJE)
Survivability and Sensor Materials Division
Materials and Manufacturing Directorate
Air Force Research Laboratory, Air Force Materiel Command
Wright-Patterson AFB, OH 45433-7750

J.T. Grant
University of Dayton Research Institute

Hao Jiang
Anteon Corporation

NOVEMBER 2004

Approved for public release; distribution is unlimited.

STINFO FINAL REPORT

MATERIALS AND MANUFACTURING DIRECTORATE
AIR FORCE RESEARCH LABORATORY
AIR FORCE MATERIEL COMMAND
WRIGHT-PATTERSON AIR FORCE BASE, OH 45433-7750

NOTICE

Using government drawings, specifications, or other data included in this document for any purpose other than government procurement does not in any way obligate the U.S. Government. The fact that the government formulated or supplied the drawings, specifications, or other data does not license the holder or any other person or corporation; or convey any rights or permission to manufacture, use, or sell any patented invention that may relate to them.

This report has been reviewed by the AFRL Wright Site Office of Public Affairs (WS/PA) and is releasable to the National Technical Information Service (NTIS). At NTIS, it will be available to the general public, including foreign nationals.

This technical report has been reviewed and is approved for publication.

//s//

Pamela M. Schaefer
Principal Materials Engineer
Technical & Strategic Planning Office
Materials and Manufacturing Directorate

Copies of this report should not be returned unless return is required by security considerations, contractual obligations, or notice on a specific document.

REPORT DOCUMENTATION PAGE

Form Approved
OMB No. 0704-0188

1. REPORT DATE *(DD-MM-YY)*	2. REPORT TYPE	3. DATES COVERED *(From - To)*
November 2004	Journal article preprint	

4. TITLE AND SUBTITLE
THE GROWTH AND CHARACTERIZATION OF PHOTONIC THIN FILMS

5a. CONTRACT NUMBER
IN-HOUSE

5b. GRANT NUMBER

5c. PROGRAM ELEMENT NUMBER
N/A

6. AUTHOR(S)
S. Tullis, W.E. Johnson, K. Eyink, P. Fleitz, and T.J. Bunning (Hardened Materials Branch (AFRL/MLPJE))
J.T. Grant (University of Dayton Research Institute)
Hao Jiang (Anteon Corporation)

5d. PROJECT NUMBER
M08R

5e. TASK NUMBER
10

5f. WORK UNIT NUMBER
00

7. PERFORMING ORGANIZATION NAME(S) AND ADDRESS(ES)

Hardened Materials Branch (AFRL/MLPJE)
Survivability and Sensor Materials Division
Materials and Manufacturing Directorate
Air Force Research Laboratory, Air Force Materiel Command
Wright-Patterson Air Force Base, OH 45433-7750

University of Dayton Research Institute

Anteon Corporation

8. PERFORMING ORGANIZATION REPORT NUMBER
AFRL-ML-WP-TP-2004-402

9. SPONSORING/MONITORING AGENCY NAME(S) AND ADDRESS(ES)
Materials and Manufacturing Directorate
Air Force Research Laboratory
Air Force Materiel Command
Wright-Patterson Air Force Base, OH 45433-7750

10. SPONSORING/MONITORING AGENCY ACRONYM(S)
AFRL/MLPJE

11. SPONSORING/MONITORING AGENCY REPORT NUMBER(S)
AFRL-ML-WP-TP-2004-402

12. DISTRIBUTION/AVAILABILITY STATEMENT
Approved for public release; distribution is unlimited.

13. SUPPLEMENTARY NOTES

ABSTRACT ***(Maximum 200 Words),*** **,**

Photonic thin films have been grown on a variety of substrates using plasma enhanced chemical vapor deposition (PECVD) of organic monomers, namely benzene and ocafluorocyclobutane (OFCB). Films produced by both homo-polymerization and co-polymerization have been prepared and analyzed. In order to introduce significant contributions from OFCB into co-polymerization films, the OFCB was introduced directly into the plasma zone and the benzene flow was reduced to a low, stable level using a high-accuracy metering valve. The films have been characterized by x-ray photoelectron spectroscopy (XPS), Fourier transform infrared spectroscopy (FTIR) and variable-angle spectroscopic ellipsometry (VASE), with an emphasis on XPS. Apart from determining the atomic composition of the films with XPS, it was extremely valuable in determining the chemistry of the films. Studies of the mechanisms of the homo-and co- polymerization reactions have aided in the fabrication of photonic films. The effects of monomer feed-in rates were applied to manipulate the composition and chemistry of the deposited films to achieve the required optical properties. Applications of PECVD to fabricate a notch filter and an anti-reflective coating are also provided.

15. SUBJECT TERMS
Thin films, XPS, FTIR, VASE, CVD, polymerization

16. SECURITY CLASSIFICATION OF:			17. LIMITATION OF ABSTRACT:	18. NUMBER OF PAGES	19a. NAME OF RESPONSIBLE PERSON (Monitor)
a. REPORT	b. ABSTRACT	c. THIS PAGE			Timothy J. Bunning
Unclassified	Unclassified	Unclassified	SAR	32	19b. TELEPHONE NUMBER *(Include Area Code)* (937) 255-3808, ext. 3167

Standard Form 298 (Rev. 8-98)
Prescribed by ANSI Std. Z39-18

THE GROWTH AND CHARACTERIZATION OF PHOTONIC THIN FILMS

J.T. Grant[1], Hao Jiang[2], S.Tullis, W.E. Johnson, K. Eyink, P. Fleitz, and T.J. Bunning

Air Force Research Laboratory, Materials and Manufacturing Directorate, Wright-Patterson Air Force Base, OH 45433, USA.
[1]Research Institute, University of Dayton, 300 College Park, Dayton, OH 45469-0168, USA.
[2] Anteon Corporation, 5100 Springfield Pike, Dayton, OH 45431, USA.

ABSTRACT

Photonic thin films have been grown on a variety of substrates using plasma enhanced chemical vapor deposition (PECVD) of organic monomers, namely benzene and octafluorocyclobutane (OFCB). Films produced by both homo-polymerization and co-polymerization have been prepared and analyzed. In order to introduce significant contributions from OFCB into co-polymerized films, the OFCB was introduced directly into the plasma zone and the benzene flow was reduced to a low, stable level using a high-accuracy metering valve. The films have been characterized by x-ray photoelectron spectroscopy (XPS), Fourier transform infrared spectroscopy (FTIR) and variable-angle spectroscopic ellipsometry (VASE), with an emphasis on XPS. Apart from determining the atomic composition of the films with XPS, it was extremely valuable in determining the chemistry of the films. Studies of the mechanisms of the homo- and co-polymerization reactions have aided in the fabrication of photonic films. The effects of monomer feed-in rates were applied to manipulate the composition and chemistry of the deposited films to achieve the required optical properties. Applications of PECVD to fabricate a notch filter and an anti-reflective coating are also provided.

Key words: Thin films, XPS, FTIR, VASE, CVD, polymerization

Corresponding author:

T.J. Bunning
Fax: +1 737 255 1128
E-mail: Timothy.Bunning@wpafb.af.mil

1. Introduction

Thin films have been used to produce anti-reflection coatings, narrow-notch filters, and high-efficiency broadband mirrors, with their performance determined by spatial control of the refractive index profiles. Usually, these films are made by depositing inorganic precursor materials using chemical vapor deposition (CVD). The large refractive index range of inorganic materials and their low absorption coefficients are the reasons that they are normally used. These materials are also suited for CVD processing, and CVD allows simultaneous deposition of two or more components in order to make special refractive index profiles. Organic materials offer several advantages over inorganic materials such as compatibility, processability, and cost, and the use of polymers as optical components is growing.

Simple one-dimensional stacks of polymer films were reported almost 20 years ago [1]. Recently, considerable activity has been centered on the use of polymer-based platforms including polymeric hydrogels [2,3], block copolymers [4,5], and organic/organic hybrids [6,7] as optical band gap materials. The success in producing one-dimensional multilayer interference films using organics lies in the refractive index difference between the materials, optical thickness control, and the number of layers that can be grown. Limitations with organics include the small range of refractive indexes and dimensional control of periodicity. Easily processed, commercial optical polymers have refractive indexes in the range of 1.4 to 1.6 [8], and thicknesses of about 75-100 nm would be required for multilayer stacks in the visible. Good thickness control at this level is therefore important.

For high, narrow notch, reflectivity, the most important factor is the refractive

index contrast [9]. The contrast can be produced in different ways, such as the classic ABAB stack or the rugate profile [10]. The rugate profile has better overall control of notch depth and width as well as increased transmission. Therefore, to produce continually varying refractive index profiles, co-deposition of high and low refractive index materials must be achievable. Plasma enhanced chemical vapor deposition (PECVD) offers the promise of dense cross-linked films with variable refractive index, and is the deposition method used in the work reported here. Plasma polymerization of organic materials is well known and many studies have been reported [11-13]. It is a dry deposition method, it is suitable for automation, the films have good adhesion with many substrates, and the surfaces do not have to be flat. Compared with conventional wet techniques, it produces very little waste. By adjusting the PECVD parameters, the chemistry and growth rate can be varied, and when depositing two precursors simultaneously a refractive index intermediate between the two starting materials is obtained.

In this work, benzene and octafluorocyclobutane (OFCB) were used as the precursor materials, benzene for a high refractive index and OFCB for a low refractive index. Thin, plasma polymerized (PP) films of each precursor were grown and characterized with x-ray photoelectron spectroscopy (XPS), Fourier transform infrared spectroscopy (FTIR) and variable-angle spectroscopic ellipsometry (VASE). The refractive indexes and composition were measured. This information was used to design and fabricate a notch filter using a multi-layer stack of PP-benzene and PP-OFCB films. Co-polymerized films were also grown and characterized. Initially, incorporation of the OFCB precursor into the films was low, but this was overcome with a change in gas inlet

position in relation to the plasma. This enabled a six-layer antireflection coating to be fabricated, showing that PECVD can be used to fabricate complex photonic film structures using organic precursors.

2. Experimental procedure

2.1 Plasma enhanced CVD reactor

A schematic of the PECVD reactor used in this work is shown in Fig.1. Argon (99.999% purity) was used as the noble gas for the plasma, and flowed at a rate of 50-200 sccm into the 10 cm diameter glass reactor at 0.66-1.3 mbar through a capacitively coupled radio-frequency (13.56 MHz) discharge between parallel plates at 5-30 W.

Vapor from HPLC grade benzene (Aldrich, purity 99.9%) was used as the high refractive index precursor, and OFCB, C_4F_8 (SynQuest, purity 99%) was used as the low refractive index precursor. The benzene reservoir was maintained at 19.0 ± 0.1 °C using a water-bath thermostat. The OFCB flow rate (0.5 – 5 sccm) was controlled using a Sierra 902C flow controller. The benzene vapor flow rate was controlled at low flow rates (0.001 – 0.5 sccm) with a manually adjusted high-accuracy metering valve, and at high flow rates (> 1 sccm) using a Sierra 902C controller. The liquid benzene and the compressed, gaseous OFCB were used without any further purification.

For growing homo-polymerized films, the precursor benzene vapor and OFCB gas were fed into the afterglow region, 7 cm downstream from the center of the plasma generation zone. The substrate was located about 1-3 cm further downstream. Films were deposited on silica, glass, silicon wafers, or IR transparent salt plates. For co-polymer

films, the OFCB was introduced directly into the plasma zone.

2.2 Characterization of the films

X-ray Photoelectron Spectroscopy (XPS) was performed using a Surface Science Instruments' M-Probe Spectrometer equipped with a monochromatic Al Kα X-ray source (energy 1486.6 eV). The surface composition for each sample was determined from survey scans taken between 0 and 1000 eV binding energy, with an analyzer pass-energy of 150 eV (corresponding to an energy resolution of about 1.5 eV). Carbon surface chemistry was determined from higher energy resolution spectra over a narrower energy range. The analysis area on the samples was 400 μm x 1000 μm.

Fourier transform infrared spectroscopy (FTIR) was used to identify the functional groups in the deposited films. Films were deposited directly onto KBr disks in the reaction chamber for FTIR analysis in the transmission mode. The FRIR analysis was performed using a Perkin-Elmer Spectrum 2000 FTIR spectrometer. A range of 400 – 4000 cm^{-1} was measured in 1 cm^{-1} steps.

Variable-angle spectroscopic ellipsometry (VASE) was used to determine the refractive index, absorption coefficient, and thickness of the films. A Woollam VASE system equipped with a VB-200 ellipsometer control unit and a CVI Instruments Digikröm 242 monochromator with 100 W mercury and 75 W xenon sources was used. Data analysis was performed using WVASE32 software. The reflected polarization states were measured over the 300 – 900 nm range in 1 nm steps and at angles of incidence of 55°, 65°, and 75°.

3. Results and discussion

3.1 Homo-polymerized films

For growing homo-polymerized films, benzene or OFCB was introduced into the afterglow region, 7 cm downstream from the plasma zone. XPS survey scans obtained from PP-benzene and PP-OFCB films are shown in Fig. 2. Note the presence of several atomic percent oxygen on the surface of the PP-benzene film. Nitrogen (~ 0.5 – 1 atomic %) was also often observed on films. The oxygen is mainly a surface contaminant formed after exposure of the film to air, possibly due to radicals retained on the surface of the polymerized film after growth. Sputtering a PP-benzene film with argon in the XPS system showed that the oxygen concentration rapidly reduced to ~ 1 atomic percent, and that the oxygen again increased after a subsequent exposure to air. The nitrogen did not change significantly, and was ~ 0.5 – 1 atomic %. This is illustrated in Fig. 3, where XPS spectra are shown (a) for a PP-benzene film, (b) after sputtering with argon for 10 min, and (c) after exposure to air for 30 min. The oxygen concentration was much lower on the surface of the PP-OFCB films (~ 0.5 -1 atomic %), as would be expected due the presence of the electronegative fluorine, Fig. 2(b). The nitrogen content was also ~ 0.5 – 1 atomic %.

The fluorine to carbon atomic concentration ratio in the OFCB films was about 1.8, slightly less than the value of 2 for the OFCB precursor, C_4F_8. However, the carbon and fluorine chemistries in the PP-OFCB film were found to be quite different from those in OFCB. This is illustrated in Fig. 4(b) where the C 1s XPS spectrum from a PP-OFCB film is shown. It can be seen that there are (at least) four peaks in the spectrum, indicating (at least) four different carbon chemistries in the film due to the four observed C 1s

binding energies. The carbon chemistries correspond to (from high to low binding energies) CF_3, CF_2, CF, and CC bonds, and the relevant concentrations of each can be obtained by curve fitting the spectrum with four peaks. Any small contribution to the C chemistry from the 0.5 – 1 atomic % oxygen or nitrogen was not included in peak fits. The fluorine concentration determined from XPS agreed very closely with that required to satisfy the intensity of the CF_3, CF_2, and CF peaks in the C 1s spectrum.

The C 1s lineshape from a PP-benzene film is shown in Fig. 4(a). Besides the main peak and its associated broad loss structure at higher binding energies (corresponding to lower electron kinetic energies), there is a shake-up peak about 7 eV on the high binding energy side of the main peak. This shake-up peak indicates a high degree of unsaturated carbon on the PP-benzene film, despite its relatively small intensity [14].

FTIR showed that the original OFCB ring structure was almost entirely destroyed during plasma polymerization, and that several different CF_x structural groups were present in the film [15]. This agrees with the XPS results obtained from the PP-OFCB film reported above. FTIR studies of the PP-benzene film showed some retention of aromatic and conjugated structures, in agreement with the XPS results.

VASE measurements showed a large difference in refractive index between the PP-benzene and the PP-OFCB films. At 632.8 nm, the refractive index of the PP-benzene film was 1.62 whereas that of the PP-OFCB was 1.37. Co-polymerized films from benzene and OFCB would then allow films with refractive indexes between these two values to be fabricated.

3.2 Co-polymerized films

Initially, when co-polymerized films using benzene and OFCB were grown, it was very difficult to include significant contributions from the OFCB into the films. Even when the OFCB flow rate was at its maximum (5 sccm) and the benzene was at its minimum (0.5 sccm), XPS showed that the fluorine concentration in the film was less than 5 atomic %. Changes in the plasma power and argon flow rate also were not effective in increasing the fluorine content. The FTIR spectrum from such a film was also very similar to the spectrum from PP-benzene, and only traces of vibrations due to CF_x groups were seen. Further, VASE showed that the co-polymerized films always had a high refractive index that was close to that from PP-benzene. Thus, there was excellent agreement between the XPS, FTIR and VASE results, in that only a small contribution from OFCB was present in the films.

Plasma co-polymerization is much more complex than homo-polymerization because of interactions between the monomers in the various stages of the reaction process, such as initiation and deposition. Because of the low contribution of OFCB when it was introduced into the afterglow region, it appears that the lower energy required to break the π-bond of benzene (2.74 eV), compared to C-F, C-H and C-C bonds (5.35, 4.30 and 3.61 eV respectively), results in a higher probability that the π-bonds of aromatic rings are more easily opened when both the benzene and OFCB are present. Also on opening the π-bond, the breaking of the C-C bond in the benzene ring is more probable than the dissociation of the C-C bond in OFCB due to the spatial hindrance of the fluorine atoms in OFCB. This is supported by the fact that PP-OFCB films have a much lower (up to 10 times) deposition rate than PP-benzene under identical conditions. Therefore, two important changes were made in an attempt to introduce higher

contributions of OFCB products into the films and allow a wide range of refractive indexes to be available for co-polymerized films. These changes were (a) to introduce the OFCB directly into the plasma zone (rather than 7 cm downstream in the afterglow region) thereby ensuring a larger quantity of CF_x reactive species due to the longer time in the plasma region, and (b) to further reduce the benzene flow rate by using a manually adjustable, high accuracy flow valve.

These two modifications allowed films to be grown with specific refractive indexes between those of PP-benzene and PP-OFCB. Two homo-polymerized films and several co-polymerized films were grown to calibrate the polymerization for sets of precursor flow rates. The flow rates of benzene and OFCB, feed ratios (defined here as benzene/(benzene + OFCB)) and the fluorine/carbon atomic ratios (from XPS) are listed in Table 1. The OFCB flow rate was between 0.5 and 3 sccm, whereas the benzene flow rate was much lower (0.004 – 0.18 sccm). The refractive indexes of the films were determined by VASE and it was found that the refractive index had a near-linear relationship on the fluorine/carbon atomic ratio. This is shown in Fig. 5, and it can be seen that the refractive index decreased from 1.62 to 1.37 as the fluorine content increased.

XPS showed that the chemistry of the films varied considerably with the monomer feed ratio, as illustrated in Fig. 6. It is obvious from this figure that plasma polymerization induces the formation of various fluorine species, including CF_3, CF_2, and CF and that these species experience relative intensity changes with the fluorine/carbon ratio in the films. These spectra were curve fit using the four components shown in Fig. 4(b), and the intensities of the CF_3, CF_2, and CF components with different monomer

feed ratios are shown in Fig. 7. The remaining intensity is from C-C, C-H and similar species. Ring breakage of OFCB produces many other reactive fluorocarbon species besides the basic structural component CF_2 due to the complicated reactions occurring during the plasma process. The CF moieties can be created from the depletion of CF_2 by liberating a fluorine atom in the plasma reaction zone [16], while the terminal group CF_3 can be formed in the gas phase by unimolecular rearrangement [17], ion-molecular collisions [18], or after film formation by ion bombardment [19]. As the benzene fraction increases, the CF_2 contribution decreases rapidly at first and then decreases more slowly. XPS shows that only about 1/3 of the fluorine content is due to CF_2 in the homo-polymerized film as compared to the starting precursor which is composed entirely of CF_2. The CF_3 component also shows a monotonic decline similar in appearance to CF_2. The CF component behaves quite differently. For the PP-OFCB film (Sample F), CF occupies about 23% of the total carbon population. With a small addition of benzene, the CF content jumps to 29% (Sample BF1), continues to increase to a maximum above 35% (sample BF3) and then begins to drop with additional benzene. Therefore, with increasing benzene content, the primary fluorine component changes from CF_2 to CF. However, the sum of the fluorine components remains nearly constant when the benzene feed share is low, close to 75%, and then decreases after the B/(B+F) ratio passes 0.004 (Sample BF3).

These XPS results are supported by FTIR results, the details of which will be published elsewhere [20]. Briefly, a comparatively broad peak spanning 1000 to 1450 cm^{-1} is due to a convolution of CF_n (n = 1-3) stretching modes, including a peak at about 1220 cm^{-1} from CF_2 vibration, one at around 1255 cm^{-1} from CF_3–CXy stretches, and one at about 1060 cm^{-1} from the CF stretch in H_2CF. The lack of any distinction between

different CF_n (n = 1-3) vibration modes implies that the films have an amorphous and disordered structure. Two small broad peaks at about 740 and 1740 cm^{-1} are attributed to vibrations from amorphous fluoro-materials, and CF-CF_3 vibrations and/or zone center CF_2 system stretching, respectively. The presence of these vibrations indicates the existence of crosslinking [21]. As the concentration of benzene increased, the characteristic features of fluorine components progressively decreased, most noticeably by the eventual disappearance of the broad peak spanning 1000 to 1450 cm^{-1}.

3.3 Fabrication of a notch filter

As mentioned above, the PP-benzene and PP-OFCB films had refractive indexes of 1.62 and 1.37 respectively. This large difference was exploited to make a multi-layer interference filter. Using these refractive indices measured from ellipsometry and deposition rates measured from experiment, a 10-bilayer stack was designed and grown by PECVD to make a notch filter. The thicknesses of the individual layers were calculated from the quarter-wavelength condition and the layers were deposited onto quartz. The transmission spectrum of the multi-layer stack is shown in Figure 8 along with the design spectrum. The positions of the peaks and the magnitude of the notch are in good agreement. This indicates good control over the deposition conditions and also that PECVD of organic precursors can be utilized to deposit optical films with good thickness control. SEM studies of the cross-section of the 10-bilayer stack show that the individual layers are dense and have good adhesion [15].

3.4 6-layer antireflection coating

Since the refractive index depends linearly on the fluorine/carbon atomic ratio (Fig. 5), films with any refractive index between the two extremes (1.62 and 1.37) can be

grown by adjusting the feed rate ratio. To demonstrate this design flexibility using PECVD, 6-layer antireflection coatings were designed for BK7 and F2 glass substrates. In these designs, the refractive index of the first layer is the same as the substrate and the other layers have gradually decreasing refractive indices, terminating with a coating of PP-OFCB. Such coatings have improved performance over single layer antireflection coatings using magnesium fluoride. An example of the improved transmission for BK7 glass is shown in Fig. 9. The uncoated glass has a transmission of 91.8 % between 400 and 700 nm, and this increased to 93.8 % between 500 and 700 nm when coated on one side. A comparison between the designed performance and the experimental result is also shown in Fig. 9. Note that this agreement is excellent above 500 nm, but the transmission drops below 500 nm due to the small absorption coefficients of the films. For F2 glass, the transmission increased from 89.5% to 93.0% after coating one side, and to 96.2% (at 600 nm) after coating both sides. The transmission of 96.2% after coating both sides of the F2 glass window was in excellent agreement with the design transmission, 96.4% [22].

4. Conclusions

The usefulness of XPS in characterizing homo-polymerized films of benzene and OFCB has been shown. XPS was also instrumental in characterizing co-polymerized films using benzene and OFCB precursors, showing that the small changes in refractive index observed were due to the inability to incorporate significant contributions from OFCB into the films when both precursors were admitted 7 cm downstream, in the plasma afterglow region. When the OFCB was introduced directly into the plasma zone, XPS showed significant contributions from OFCB components in the films and the

refractive index could now be varied between those of PP-benzene and PP-OFCB by adjusting the feed rate ratio. XPS was also used to characterize the CF_x components in the films. The complementary nature of XPS, FTIR and VASE has also been illustrated. Finally, applications of PECVD to grow a notch filter and an anti-reflective coating were demonstrated, and good experimental agreement with the coating designs was obtained.

References

[1] Alfery T, Gurnee EF, Schrenk WJ. Polym Eng Sci 1986; 9: 400.

[2] Xu X, Friedman G, Hunfeld KD, Majetich SA, Asher SA. Adv Mat 2001; 13: 1681.

[3] Rundquist PA, Photinos P, Jagannathan S, Asher SA. J Chem Phys 1989; 91:4932.

[4] Edrington AC, Urbas AM, DeRege P, Chen CX, Swager TM, Hadjichristidis N, Xenidou M, Fetters LJ, Joannopoulos JD, Fink Y, Thomas EL. Adv Mater 2001; 13: 421.

[5] Fink Y, Urbas AM, Bawendi MG, Joannopoulos JD, Thomas EL. J Lightwave Tech 1999; 17: 1963.

[6] Hart SD, Maskaly GR, Temelkuran B, Pridaux PH, Joannopolous JD, Fink Y. Science 2002; 296: 510.

[7] Fink Y, Winn JN, Fan S, Chen C, Michel J, Joannopoulos JD, Thomas EL. Science 1998; 282: 1679.

[8] Mark JE, Physical Properties of Polymers Handbook, Woodbury, NY, American Institute of Physics, 1996.

[9] Macleod HA, Thin-Film Optical Filters, New York, Macmillan Publishing Company, 1986.

[10] Johnson WE, Crane RL. SPIE Proc 1993; 2046: 88.

[11] Yasuda H. Plasma Polymerization, New York, Academic Press, 1985.

[12] Denes F. Trends Polym Sci 1997; 5: 23.

[13] Shi F. Surf Coatings Tech 1996; 82: 1.

[14] Beamson G, Briggs D. High Resolution XPS of Organic Polymers; The Scienta ESCA300 Database, Chichester, UK, John Wiley & Sons, 1992.

[15] Jiang H, Johnson WE, Grant JT, Eyink K, Johnson EM, Tomlin DW, Bunning T. Chem Mater 2003; 15: 340.

[16] Bretagne J, Epaillard F, Ricard A. J Polym Sci: Pt A: Polym Chem 1992; 30: 323.

[17] Budzikiewiz H, Djerassi C, Williams DH. Mass Spectrometry of Organic Compounds. San Francisco: Holden-Day, 1967.

[18] Lias SG. In: Roots JW, editor. Fluorine-containing free radicals. Washington, DC: American Chemical Society, 1978.

[19] O'Keefe MJ, Rigsbee JM. J Appl Polym Sci 1994;53:1631.

[20] Jiang H, Grant JT, Tullis S, Eyink K, Johnson WE, Fleitz P, Bunning T. in submission.

[21] Mackie NM, Dalleska NF, Castner DG, Fisher ER. Chem. Mater. 1997; 9: 349.

[22] Jiang H, O'Neill K, Grant JT, Tullis S, Eyink K, Johnson WE, Fleitz P, Bunning T. Chem Mater 2004; 16: 1292.

Table 1: OFCB and benzene feed volume rates and the (fractional) monomer feed ratios during plasma homo-polymerization and co-polymerization, and the fluorine/carbon atomic ratios of the grown films determined by XPS. For the monomer feed ratio, B is benzene feed rate and F is the OFCB feed rate.

Sample	OFCB feed rate (sccm)	Benzene feed rate (sccm)	Monomer feed ratio {B/(B+F)}	Fluorine/Carbon atomic ratio (F/C) in the films
Homopolymer film of benzene (Sample B)	0	0.177	1	0
Copolymer film BF9	0.5	0.177	0.261	0.23
Copolymer film BF8	2.5	0.177	0.0661	0.46
Copolymer film BF7	3	0.177	0.0557	0.47
Copolymer film BF6	3	0.079	0.0257	0.60
Copolymer film BF5	3	0.040	0.0132	0.62
Copolymer film BF4	3	0.013	0.00431	0.81
Copolymer film BF3	3	0.012	0.00398	0.96
Copolymer film BF2	3	0.010	0.00332	1.25
Copolymer film BF1	3	0.004	0.00133	1.36
Homopolymer film of OFCB (Sample F)	3	0	0	1.62

Figure captions

Fig. 1. Schematic diagram of the plasma enhanced chemical vapor deposition system. For the homo-polymerized films, the OFCB is introduced downstream where the interaction is with metastable argon ions in the flowing afterglow region. For co-polymerized films, the OFCB is introduced directly into the plasma zone.

Fig. 2. XPS survey spectra of (a) a PP-benzene film and (b) a PP-OFCB film.

Fig. 3. XPS spectra are shown (a) for a PP-benzene film, (b) after sputtering with argon for 10 min, and (c) after exposure to air for 30 min.

Fig. 4. C 1s spectra from (a) a PP-benzene film showing the shake-up peak, and (b) a PP-OFCB film showing the effect of fluorine chemistry.

Fig. 5. The refractive index at 632.8 nm as a function of the fluorine/carbon atomic ratio in the deposited films.

Fig. 6. C1s spectra from four of the PECVD films. At the bottom is the spectrum of a plasma homo-polymerized OFCB film (Sample F). Then, there are two spectra of the plasma copolymerized films (Samples BF3 and BF7) in order of increasing benzene in the monomer feed ratio (B/(B+F)) from bottom to top, and at the top, the spectrum of a plasma homo-polymerized benzene film (Sample B). The spectra have been normalized and offset for clarity.

Fig. 7. The variations of the structural species CF_3, CF_2, and CF in the plasma homo-polymerized and co-polymerized films are shown in parts (a), (b), and (c), respectively, as a function of monomer feed ratio, B/(B+F).

Fig. 8. Comparison of the transmission spectrum of the multi-layer homo-polymer stack (dotted line) together with the design spectrum (solid line).

Fig. 9. Transmission for a single-sided 6-layer co-polymer antireflection coating on BK7 glass ♦, compared to the coating design ■ , and the uncoated glass ●.

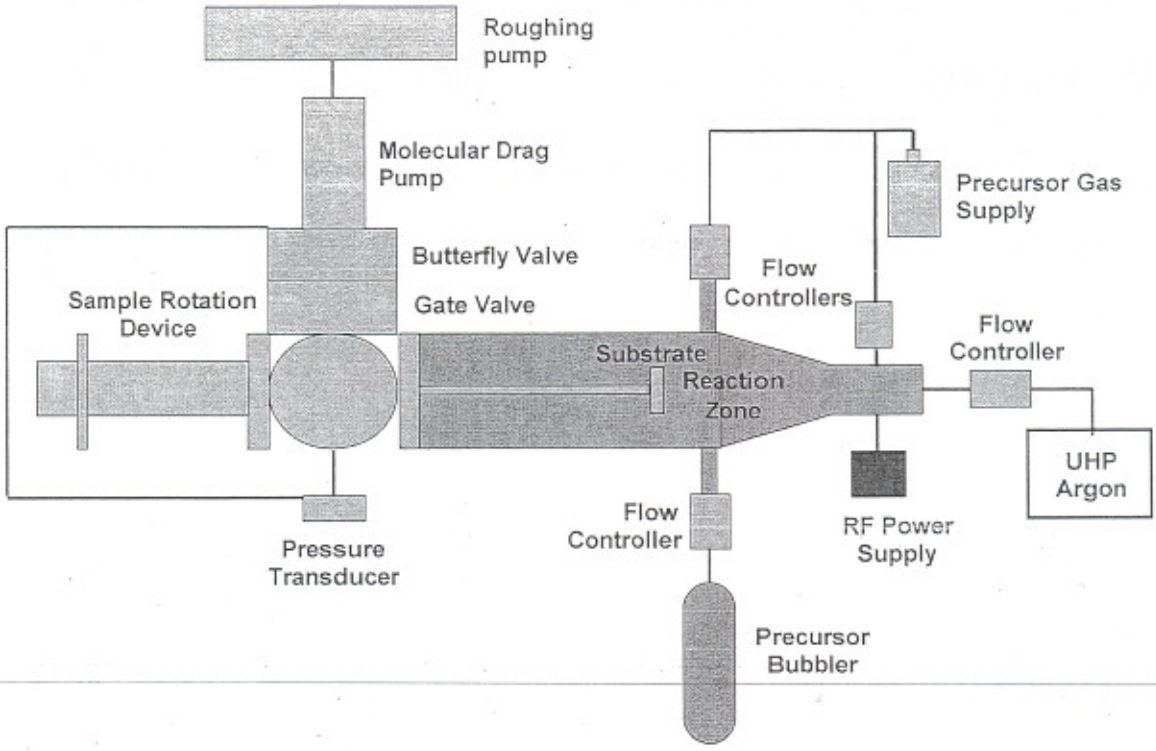
Roughing pump
Molecular Drag Pump
Butterfly Valve
Gate Valve
Sample Rotation Device
Substrate
Reaction Zone
Flow Controllers
Precursor Gas Supply
Flow Controller
UHP Argon
RF Power Supply
Flow Controller
Precursor Bubbler
Pressure Transducer

Fig. 1.

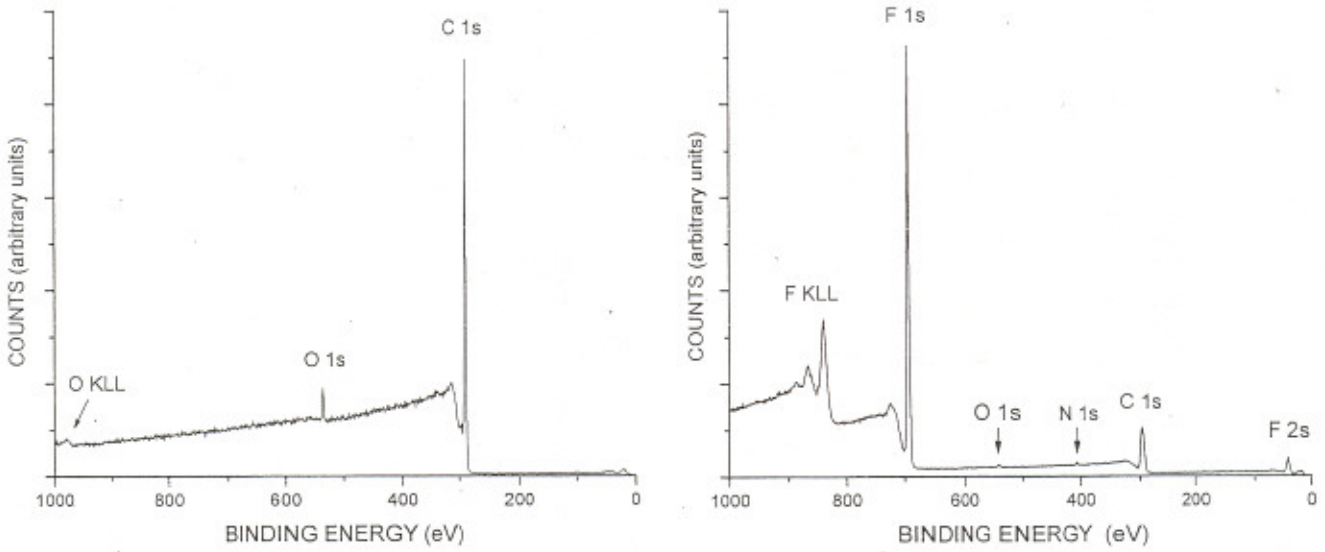
C 1s
COUNTS (arbitrary units)
O KLL
O 1s
1000
800
600
400
200
0
BINDING ENERGY (eV)
F 1s
F KLL
O 1s
N 1s
C 1s
F 2s
COUNTS (arbitrary units)
1000
800
600
400
200
0
BINDING ENERGY (eV)

(a) (b)

Fig. 2.

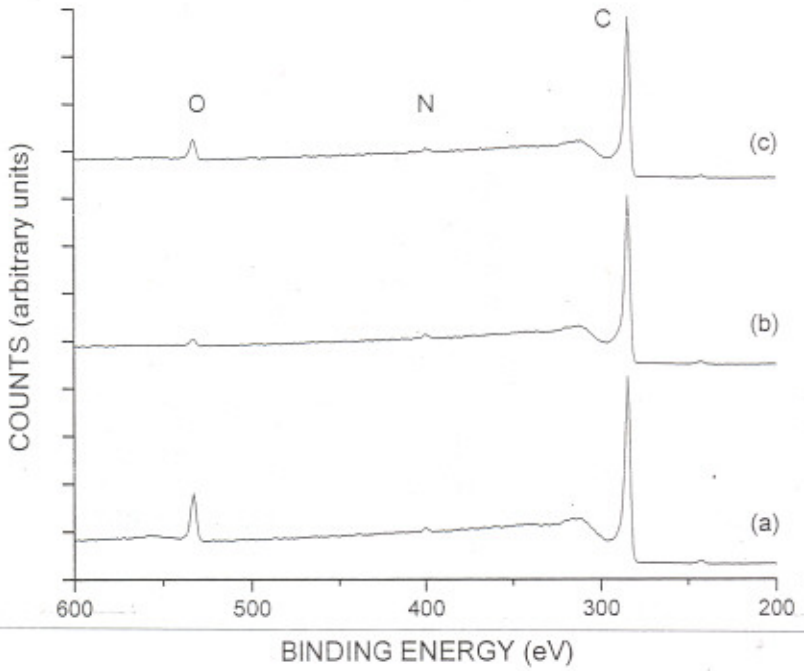
C
O
N
(c)
(b)
(a)
COUNTS (arbitrary units)
600
500
400
300
200
BINDING ENERGY (eV)

Fig. 3.

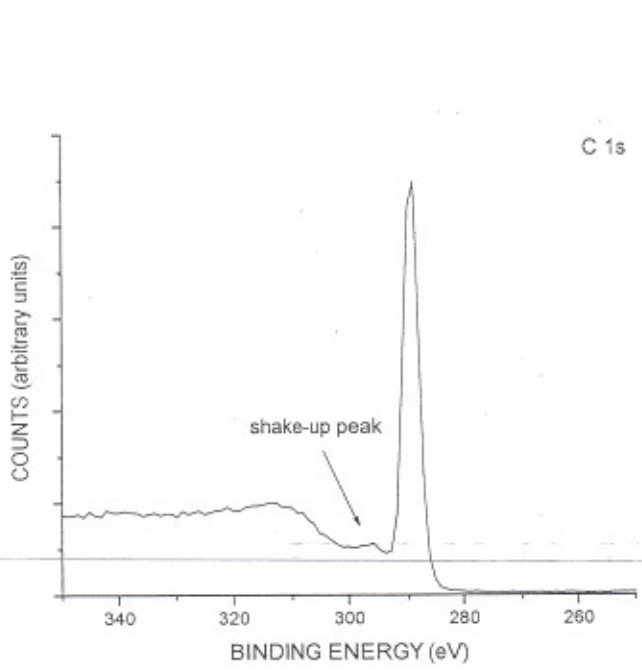
C 1s
COUNTS (arbitrary units)
shake-up peak
340
320
300
280
260
BINDING ENERGY (eV)

(a)

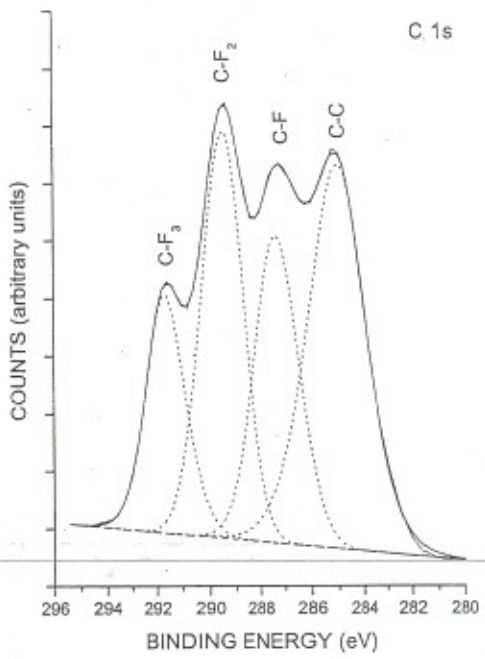
C 1s
C-F3
C-F2
C-F
C-C
COUNTS (arbitrary units)
296
294
292
290
288
286
284
282
280
BINDING ENERGY (eV)

(b)

Fig. 4.

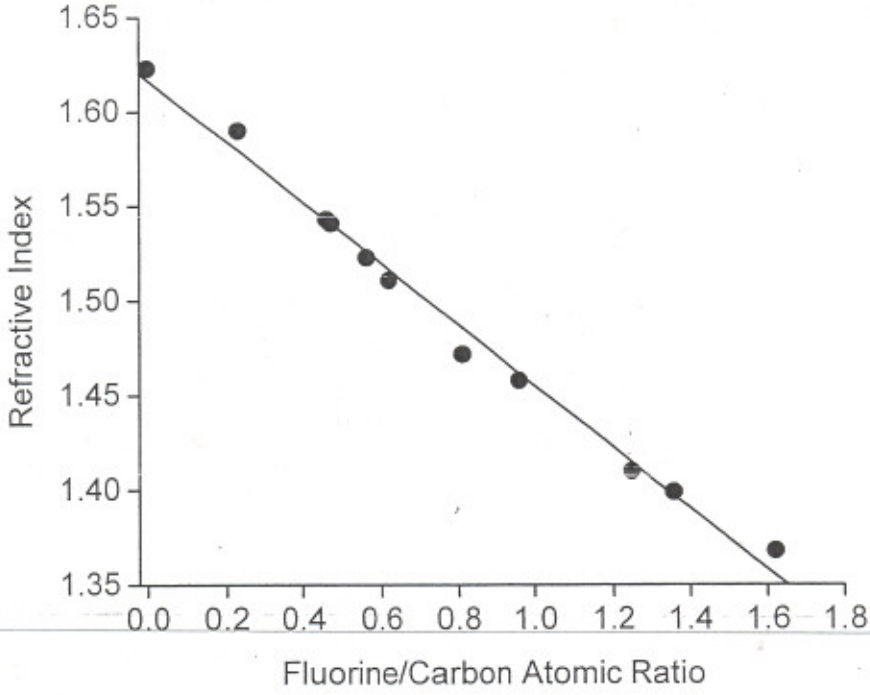
Refractive Index
1.65
1.60
1.55
1.50
1.45
1.40
1.35
0.0
0.2
0.4
0.6
0.8
1.0
1.2
1.4
1.6
1.8
Fluorine/Carbon Atomic Ratio

Fig. 5.

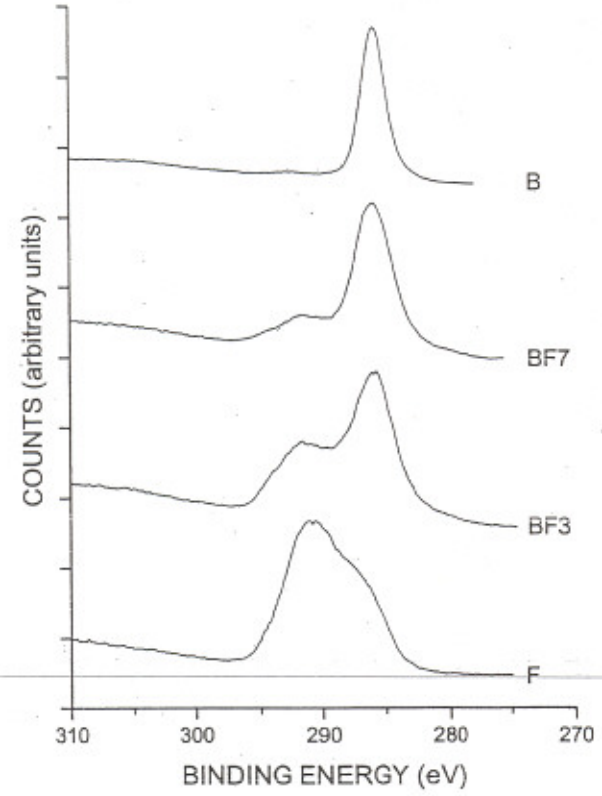
COUNTS (arbitrary units)
B
BF7
BF3
F
310
300
290
280
270
BINDING ENERGY (eV)

Fig. 6.

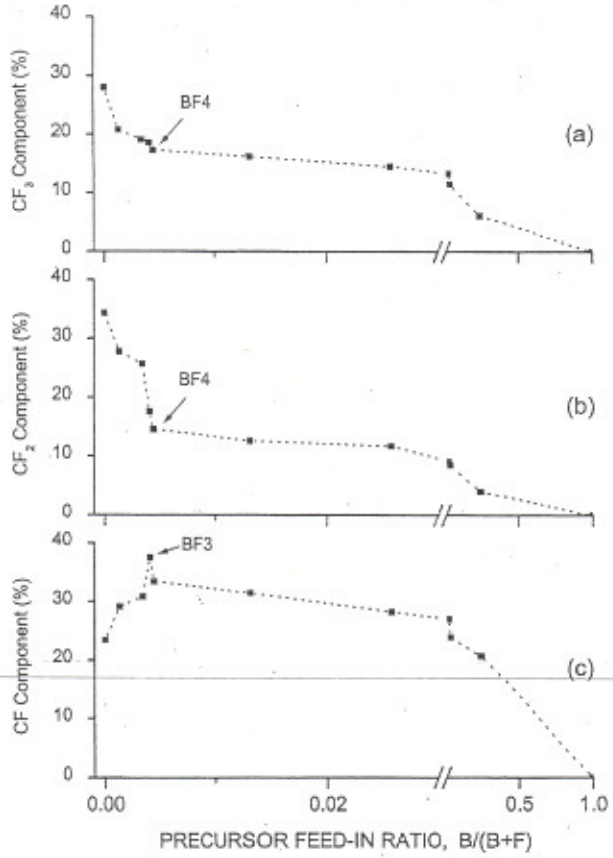
40
30
20
10
0
CF_3 Component (%)
BF4
(a)
CF_2 Component (%)
BF4
(b)
CF Component (%)
BF3
(c)
0.00
0.02
0.5
1.0
PRECURSOR FEED-IN RATIO, B/(B+F)

Fig. 7.

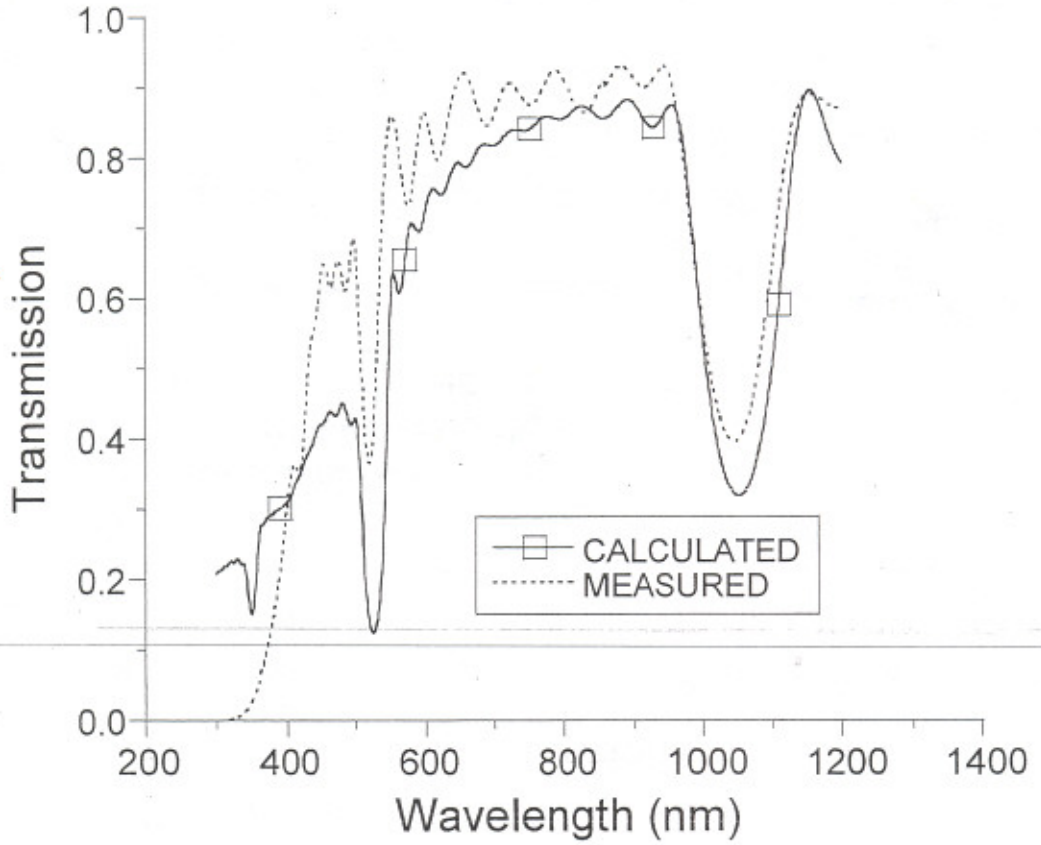
1.0
0.8
0.6
0.4
0.2
0.0
Transmission
200
400
600
800
1000
1200
1400
Wavelength (nm)
CALCULATED
MEASURED

Fig. 8.

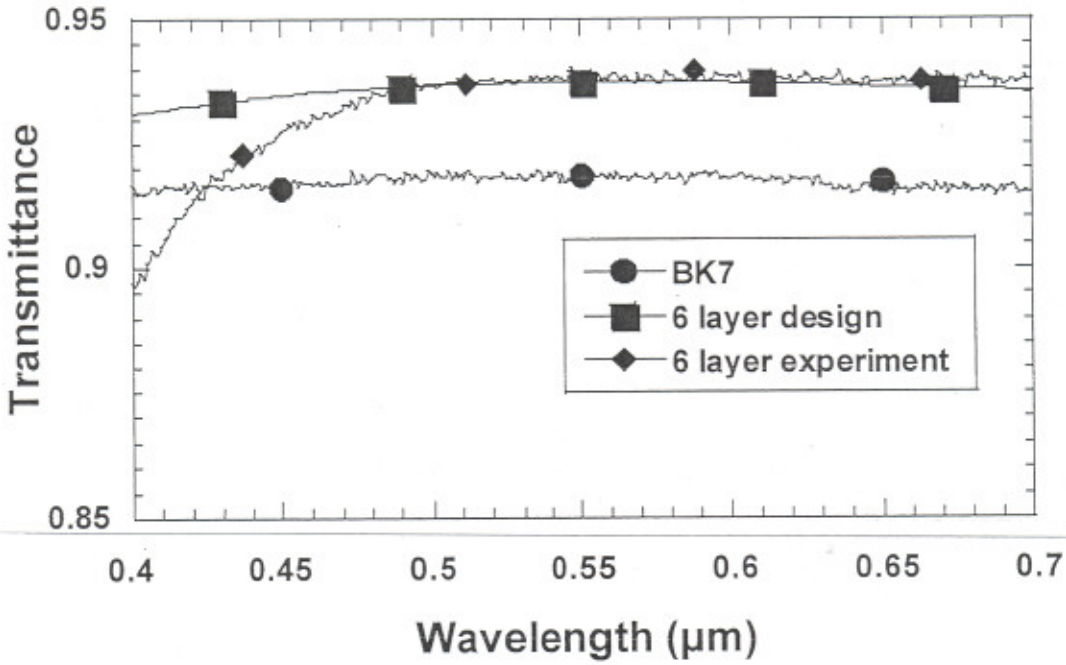
0.95
0.9
0.85
Transmittance
0.4
0.45
0.5
0.55
0.6
0.65
0.7
Wavelength (μm)
BK7
6 layer design
6 layer experiment

Fig. 9.